International Journal of Plasticity xxx (2010) xxx–xxx

Contents lists available at ScienceDirect

International Journal of Plasticity

journal homepage: www.elsevier.com/locate/ijplas

Determination of constitutive response of plastically graded materials

Nathan A. Branch, Nagaraj K. Arakere *, Ghatu Subhash, Michael A. Klecka

Department of Mechanical and Aerospace Engineering, University of Florida, Gainesville, FL 32611-6300, United States

ARTICLE INFO

Article history:
Received 25 April 2010
Received in final revised form 3 September 2010
Available online xxxx

Keywords:
Vickers indentation
Constitutive response
Finite element analysis
Plastically graded material
Hardness

ABSTRACT

Plastically graded materials (PGMs) are frequently used in high-performance tribological components such as case-hardened gears and bearings for jet and rocket engines due to their superior resistance to rolling contact fatigue. These components can have a surface hardness as high as 9 GPa and a decreasing hardness gradient over a depth of approximately 2 mm. This hardness gradient is achieved by a gradient in carbon content. Proper design of such components requires the knowledge of the constitutive response with depth. In this manuscript, a coordinated experimental and numerical method is presented to extract the constitutive response of commercially available case-hardened Pyrowear 675 (P675) stainless steel. Utilizing the variation in micro-Vickers hardness with depth for both virgin and plastically deformed PGMs, representative plastic strain, and well established hardness-yield strength relationships, the constitutive response of the PGM is uniquely determined. It is shown that this specific PGM has a linear variation in yield strength, but a constant strain hardening exponent. The procedure developed here can assist in surface engineering a PGM with optimized hardness profiles to maximize tribological performance.

1. Introduction

Incorporation of gradients in material microstructure to tailor the functional properties of engineering materials has been in use since the iron-age (Smith, 1960). Such graded materials were heat treated to obtain a surface that is harder than its core for use in weapons such as swords, spears, and shields (Suresh and Mortensen, 1998; Miyamoto et al., 1999). Interestingly, these principles of heat treatment are still practiced throughout the steel industry even in today's advanced-technology applications. Plastically graded materials (PGMs) traditionally have constant elastic properties while the plastic response varies with depth (Cao and Lu, 2004; Choi et al., 2008a,b), whereas a variation in elastic modulus is also possible for some materials (Gu et al., 2003; Fischer-Cripps, 2003). The variation in plastic response can be achieved either by variation in material microstructure, material composition, or a combination of both. In many case-hardened steels the variation in plastic response with depth is accomplished by heat-treating the outer surface through carburizing, nitriding, or boriding (Boyer, 1987) to obtain a microstructure with high hardness on the surface and a gradual reduction in hardness with depth. Such materials are used for the manufacture of high-performance tribological components such as ball and roller bearing raceways and gears for aircraft and space propulsion turbine engines. The decreasing hardness profile of the case-carburized PGM with depth is designed to take advantage of the decreasing plastic strain amplitudes induced by rolling contact fatigue (RCF). The hardness gradient within the case layer can be indicative of complex variations in yield strength and work hardening behavior with depth. Determination of the monotonic and cyclic stress–strain response of such

* Corresponding author. Tel.: +1 352 392 0856; fax: +1 352 392 1071.
E-mail address: nagaraj@ufl.edu (N.K. Arakere).

0749-6419/$ - see front matter © 2010 Elsevier Ltd. All rights reserved.
doi:10.1016/j.ijplas.2010.09.001

plastically graded materials is essential to improve the RCF life of tribological materials with tailored properties for many high-performance applications.

Evaluation of graded material properties through indentation has gained considerable attention in recent years. Fischer-Cripps (2003) used instrumented ball indentation and finite element analysis to determine the elastic modulus variation in elastically graded materials. However, most graded engineering materials have a variation in plastic properties as well. Nakamura et al. (2000) implemented instrumented ball indentation and Kalman filtering techniques to estimate the variation in plastic response of PGMs and used a standard rule of mixtures to determine the stress and strain contributions from metal and ceramic portions of the PGM. A set of PGM indentation reference behavior was created by many FE model simulations, and experimental verification of this method was conducted by Gu et al. (2003). Giannakopoulos (2002) implemented analytical and numerical methods to analyze the deformation induced by sharp indentation of PGMs, but this was limited to nonlinear elastic and perfectly plastic materials. Nayebi et al. (2002) predicted the decreasing hardness profile of nitrided steels using instrumented ball indentation and finite element analysis. Cao and Lu (2004) used finite element analysis to simulate conical indentation of PGMs and the resulting load–displacement curves were used in a reverse analysis to predict their plastic response. It was found that the indentation loading curvature can vary with indentation depth for a PGM. Choi et al. (2008a,b) analyzed the influence of yield strength gradient of a PGM on indentation loading curvature, distribution of maximum principal and von Mises stresses, and equivalent plastic strain gradient within the plastic zone of a conical indent. They used dimensionless functions to describe the indentation loading curvatures of homogeneous elastic materials (Johnson, 1985) and non-graded elastic–plastic materials (Dao et al., 2001) to create a new dimensionless function that describes the indentation loading curvature of PGMs. Experimental validation was conducted on graded materials processed by electro-deposition techniques which resulted in a variation in grain size and consequently, yield strength (Choi et al., 2008a,b). Cordill et al. (2009) present interesting results on dynamic indentation methods for measuring mechanical properties for bulk and thin film materials and show that the alteration in hardness during shallow indentation is due to the added energy associated with the oscillation which assists dislocation nucleation. Haji-Ali et al. (2008) present an artificial neural networks approach to simulate nanoindentation response of a variety of materials with nonlinear behavior using the monotonic loading part of the load-deflection response to extract material properties. The indentation of strain hardening materials with decreasing hardness gradients was investigated by Zhang et al. (2007). Anand and Ames (2006) present a new continuum model for the viscoelastic–plastic deformation of amorphous polymeric solids for extracting material property information using micro-indentation. Most of the above investigations were focused on how variations in plastic response affected the indentation loading curvature of PGMs. None of them, however, used a plastically deformed PGM to relate its increase in hardness to the corresponding flow curve that will vary with depth. The method presented here will utilize the actual plastic deformation within the plastic zone created by Vickers indentation to determine the gradient in plastic response.

Due to the unique graded microstructure of PGMs, it is possible to use gradient plasticity theories to analyze these materials. Such theories focus on geometrically necessary dislocations which give rise to nonlocal and size effects (Fleck et al., 1994; Fleck and Hutchinson, 2001; Huang et al., 2004). While this approach may indeed provide new insights into the evolving plastic strain gradients in a PGM, in this manuscript the authors aim to model the plastic response using the classical plasticity model. Nevertheless, it will be shown here that this approach is effective in capturing the experimentally observed trends in the hardness gradients of a plastically deformed PGM. It is cautioned here that the term 'plastic strain gradient' here refers to the spatial variation of plastic strain within the deformed zone and should not be confused with terminology surrounding strain gradient plasticity which investigates the effects of strain gradients on constitutive modeling.

A coordinated experimental and numerical approach utilizing macro and micro-indentations and elastic–plastic finite element analysis (FEA) is presented in this study to determine the variation in constitutive response of a PGM that is widely used in high-performance aerospace bearings and gears. The PGM utilized here has a variation in plastic response with depth, but constant elastic modulus. The fact that a strain hardening material exhibits increased indentation hardness due to plastic deformation compared to its virgin hardness is utilized here in both the measurement and prediction of Vickers hardness for a relatively large magnitude and range of plastic strains (ε_p) within a PGM. A convenient and controlled way to induce large magnitudes of plastic strain within a PGM is via macro-Vickers indentation which causes (Fig. 1) symmetric plastic strain about its centerline line. Within this plastic zone, the material will strain harden according to its plastic response and consequently display an increase in indentation hardness with respect to its virgin state. The principal concept of this analysis is that the increase in hardness (converted to flow stress through a modified Tabor's rule (Tabor, 1970; Branch et al., in press-a) at a given depth with respect to its virgin state *must fall on the flow curve* defined at that depth as depicted in Fig. 1 where stress strain curves at two depths are depicted and related to the hardness measurements at these locations. Because the material is plastically graded with depth, the stress–strain response is noted to be different at each depth. While the hardness measurements on virgin material only provide information on virgin yield stress as per Tabor's relationship, to determine the plastic response of the material, a macro indentation is conducted to create large plastic deformation within the PGM. The increase in hardness within this plastic zone is experimentally measured by micro-Vickers indentations which are then compared to those predicted by finite element models described later. The *micro*-indents ($\approx$ 200 g) essentially probe the increase in local yield strength within the plastic zone of the *macro*-indent (>150 Kg). The increase in yield strength can be predicted by finite element modeling provided the appropriate flow curves are used at every point throughout the PGM. The increase in yield strength will correspond to a certain amount of plastic strain which is dependent on the strain hardening characteristics of the flow curve at that depth. As an example, for a PGM with decreasing hardness with depth (Fig. 1)

Please cite this article in press as: Branch, N.A., et al. Determination of constitutive response of plastically graded materials. Int. J. Plasticity (2010), doi:10.1016/j.ijplas.2010.09.001

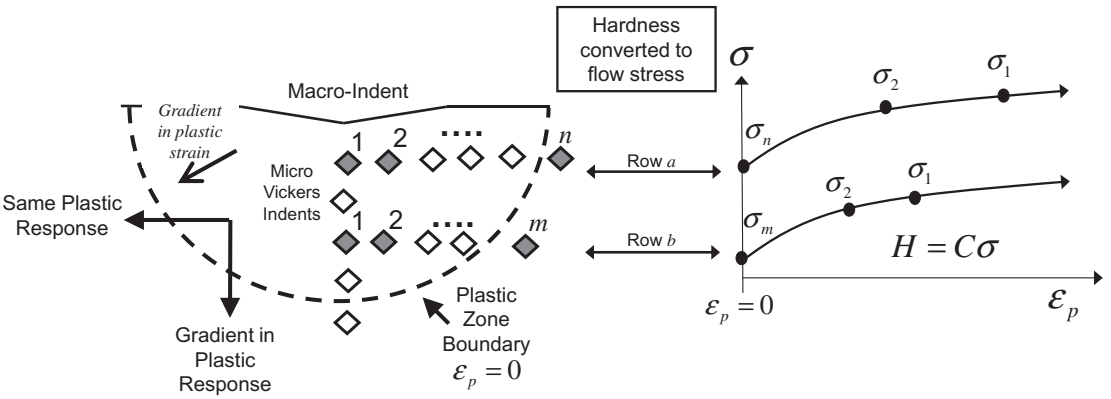

Fig. 1. Schematic of the relationship between indentation hardness and plastic response at any given depth within the plastic zone of a PGM.

the flow stress is expected to decrease with depth because the hardness is a measure of yield strength (Tabor, 1970). Thus the new micro-hardness measurements within the plastically deformed zone will provide the increase in flow stress at a specific depth. These flow stress values must fall on the flow curve defined for the material at that depth. Outside of the plastic zone, any hardness measurements will reflect the virgin (undeformed) material yield strength at that depth. For instance, the hardness measurement at location *n* in Fig. 1 will probe the yield strength of a virgin region because it is outside of the plastic zone caused by the macro-indent. The hardness measurements along Row *a* are expected to be higher than the hardness at *n* due to the strain-hardening of the material within the plastic zone, while keeping in mind that the flow stresses for any material point along Row *a* must fall on the same flow curve as that at point *n*. The same holds true for Row *b* and point *m*, but the magnitudes would be lower due to the decreasing hardness trend in this PGM example. This information, along with the corresponding plastic strain obtained from FE models, will be utilized to determine the variation in plastic response with depth for a commercially available PGM.

2. Material

Commercially available P675 case-hardened stainless steel is used in the current study. Prior to carburization and heat treatment, the steel contains only 0.1% carbon. After carburization, the surface of the case-hardened layer can contain up to 1% carbon which decreases with depth due to the carbon diffusion process. Additional heat treatment involving double-tempering is used to lock in the final microstructure which consists of tempered martensite and dispersed carbide particles less than 2 μm in size. The variation of carbide particle volume fraction with depth results in a variation in hardness and plastic response over the case-hardened region. To determine the variation in virgin hardness with depth within this specific PGM, the samples were sectioned, ground, and polished on surfaces parallel to the carbon gradient. Standard metallographic polishing procedures which use progressively finer polishing media were used to minimize damage and residual stresses induced by polishing. Micro-Vickers indentations were conducted on this cross-section using a Wilson® Instruments (Tukon™ 2100B) Vickers indenter at 200 g, 500 g, and 1 Kg indent loads for 15 s loading duration. The indents were spaced 2.5 times the indent diagonal to prevent interactions with neighboring indents as per ASTM E384 standard. The micro-Vickers hardness versus depth profile shown in Fig. 2 for the virgin P675 steel depicts negligible indentation size effect (ISE) for this chosen indent load range (Abu Al-Rub and Voyiadjis, 2004; Qu et al., 2006). At indent loads lower than 200 g ISE will as observed, but such low indent loads were avoided here as the size of the indents become difficult to measure using an optical microscope. ISE is also dependent on the grain size of the material, which was approximately 2 μm for the case-hardened steel used in this analysis. The typical size of the indentation diagonal at a load of 200 g is around 20 μm which is significantly greater than the grain size and hence the ISE is not seen. The plot in Fig. 2 reveals that hardness varies linearly from 930 Hv at the surface to 433 Hv over a depth of 2 mm, after which the hardness remains constant in the core region. The graded region in hardness will be the PGM of interest for this investigation. The plastic response of the core, non-graded region will be obtained by a traditional compression test. The resulting plastic response is considered to be representative of the PGM's softest region and provides a lower bound of possible plastic behavior for the entire PGM.

3. Experimental procedure

To induce a large plastic strain within the graded material, macro-Vickers indents were produced at large loads (up to 330 Kg) using a standard Vickers indenter. The indenter was fixed in a custom housing and mounted in a Universal Testing Machine load frame (MTS Alliance™ RT/30) and driven in load control for 15 s. A macro-Vickers indent was conducted on the hardest surface (930 Hv, 'H' in Fig. 2) of the PGM in the direction of decreasing hardness, (i.e. hard to soft). It will be shown that the resulting plastic zone from this macro-indent was not deep enough to plastically deform the entire graded material

Please cite this article in press as: Branch, N.A., et al. Determination of constitutive response of plastically graded materials. Int. J. Plasticity (2010), doi:10.1016/j.ijplas.2010.09.001

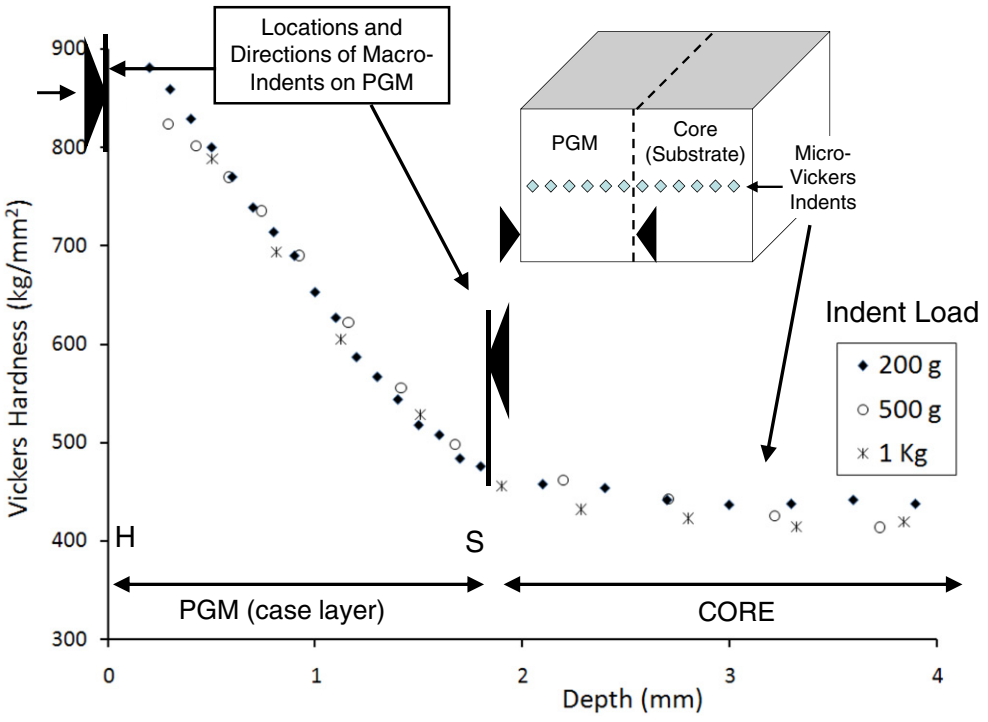

Fig. 2. Variation in micro-Vickers hardness with depth within a virgin P675 graded material. Three different indent loads show very little indentation size effect (ISE). 'H' and 'S' refer to the hardest and softest regions, respectively, of the PGM.

and therefore an essentially new PGM was created by removing the soft core region and polishing up to the graded region with new surface hardness of 500 Hv ('S' Fig. 2) in the direction of increasing hardness, (i.e. soft to hard). These two PGMs will be used to demonstrate the validity of the proposed method for determining the plastic response of a PGM with both increasing and decreasing gradients in hardness and allow for most of the case-hardened region to be plastically deformed. The macro-Vickers indents (Fig. 2) were sectioned and polished up to the indent diagonals (Fig. 3) which correspond to the maximum indent and plastic zone depths. Standard metallographic polishing procedures were used to prevent residual stress accumulation and additional plastic deformation induced by polishing. *Micro*-Vickers indents were then conducted on these cross-sections at 200 grams load and 100 μm spacing to measure the increase in hardness within the plastic zone of the *macro*-Vickers indent. Micrographs of the micro-Vickers indents of the cross sections of the hardest and softest macro-

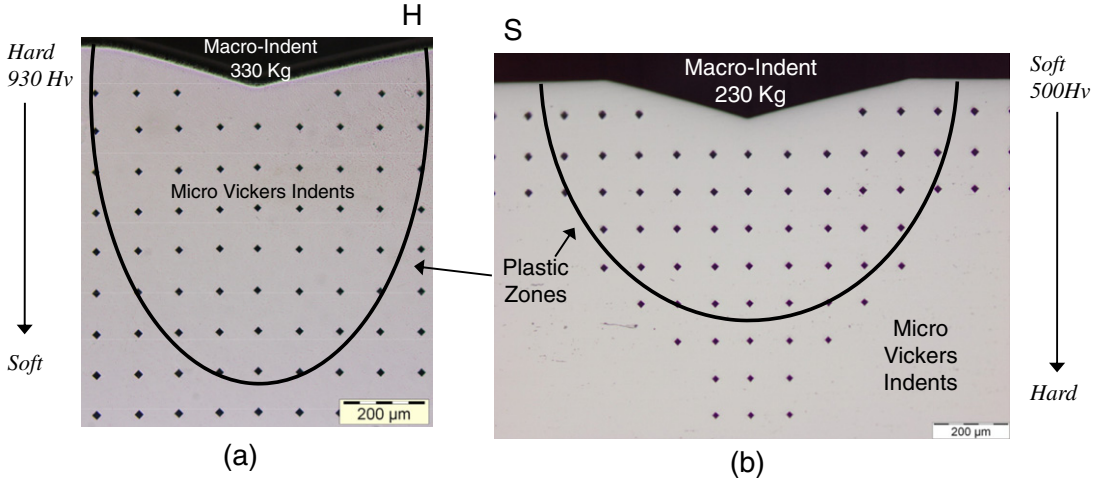

Fig. 3. Micro-Vickers indent (200 g) map within plastic zone induced by the macro-Vickers indention on (a) the hardest and (b) softest surfaces of the PGMs. Notice smaller microindent sizes within the hardest region.

Please cite this article in press as: Branch, N.A., et al. Determination of constitutive response of plastically graded materials. Int. J. Plasticity (2010), doi:10.1016/j.ijplas.2010.09.001

indents are shown in Fig. 3a and b, respectively. The variation in hardness can be seen visually in Fig. 3 where the micro-indent sizes change along the cross-section. Because the indent load is the same for all micro-indents, the hardest regions have smaller indent sizes when compared to the softest regions. This method of micro-indent mapping below a macro indent is similar to the approaches adopted by Srikant et al. (2006), Chaudhri (1998), Koeppel and Subhash (1999), but will be extended here to predict the flow curves of a PGM. The plastic zone boundaries shown in Fig. 3 were estimated from the increased hardness measurements relative to their virgin state outside of the plastic zone.

The macro-Vickers indentation on the hardest PGM surface (Fig. 3a) was created by an indent load of 330 Kg which resulted in an average macro indent diagonal length of 800 μm. The increase in micro-Vickers hardness along the centerline of the plastic zone is depicted in Fig. 4a. The maximum increase in hardness is approximately 50 Hv for the indent closest to the surface and decreases to the virgin hardness trend at the plastic zone boundary. If this region had a perfectly plastic response with depth, there would have been no strain hardening, no increase in flow stress, and consequently no increase in hardness within the plastic zone of the macro-indent. Thus the increase in hardness within the plastic zone is dependent on material strain hardening properties and the magnitude of plastic strain. As per the ASME E384 standard, the indents must be at least 100 μm from the surface. The maximum depth of the macro indent tip was 150 μm Thus, for the material point that was closest to the tip of the macro indent, the first measurable point where the data was available was around 250 μm from the original (undeformed) surface.

A similar procedure was conducted on the softest PGM surface that has an increasing subsurface hardness trend with depth (Fig. 3b). The macro-indent on the softest surface (500 Hv) was conducted at a reduced load of 230 Kg but resulted in a larger indent diagonal of 940 μm. As before, the increase in hardness along the centerline of the plastic zone is shown in Fig. 4b. The maximum increase in hardness is again approximately 50 Hv in the region of large plastic strain and decreases to zero at the elastic–plastic boundary. The increase in hardness within the plastic zones of both PGMs is indicative of the material's ability to strain-harden. The question yet to be answered, however, is what equivalent plastic strain magnitude corresponds to the above measured hardness (flow stress) values? To answer this question, these macro-Vickers indentation experiments of graded materials are simulated in finite element models. The flow curve variation with depth will be estimated from the flow curve of the core region and the variation in hardness with depth within the PGM. The measured increase in micro-hardness within the plastic zone of the macro-indent will be estimated from the equivalent plastic strain calculated by the FE model.

4. Constitutive response

The variation in microstructure with depth within the case-hardened region results in a variation in yield strength and plastic response. Determining the constitutive response of any given point within the PGM using traditional methods such as a tension and compression test is impractical because of the difficulty in preparing a specimen of uniform composition that corresponds to any given point within the PGM. However, the core region has uniform microstructure and hardness (Fig. 2), and the ample amount of core material available allows for a compression test specimen of 10 mm × 6 mm × 3.175 mm to be extracted. The compression test was conducted in a MTS load frame. The power-law curve fit, $\sigma = K\varepsilon^n$, applied to the flow curve obtained from this compression test shown in Fig. 5 resulted in a strength coefficient K = 1800 MPa and a strain hardening exponent n = 0.064. Because this is the softest region of the PGM, this information provides a lower bound of possible plastic behavior for the entire PGM.

Because the *increase* in hardness was approximately constant within the plastically deformed PGMs, it is reasonable to assume that the value for n remains constant throughout the PGM. This assumption will be later validated by the mechanistic approach presented here which is based on well established concepts such as representative plastic strain (Tabor, 1970)

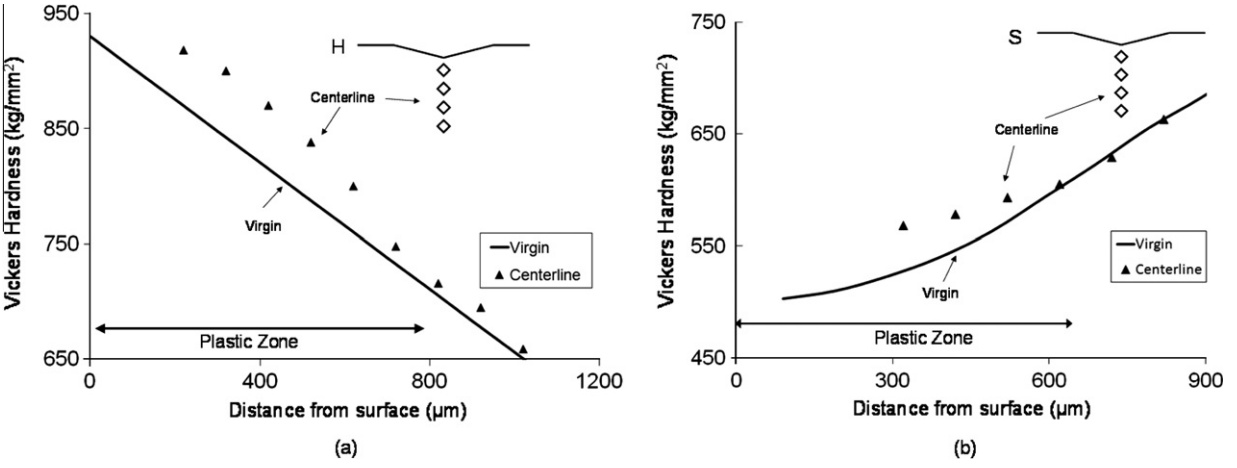

Fig. 4. Experimentally measured micro-Vickers hardness along the centerline of the macro indent for (a) hardest and (b) softest PGM surfaces.

Please cite this article in press as: Branch, N.A., et al. Determination of constitutive response of plastically graded materials. Int. J. Plasticity (2010), doi:10.1016/j.ijplas.2010.09.001

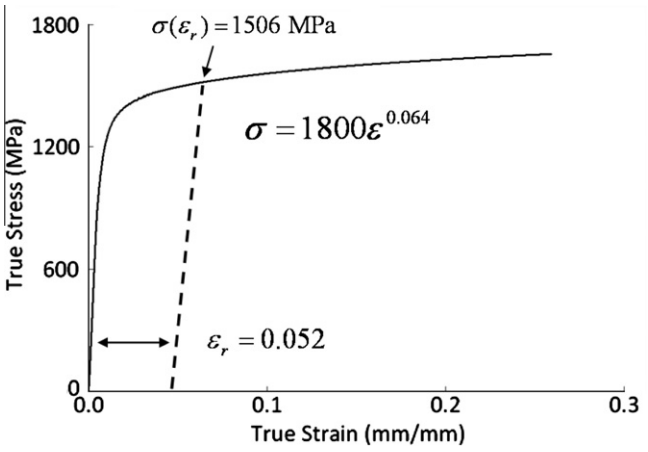

Fig. 5. Flow curve obtained from compression test of the homogeneous core.

and constraint factor (Gao et al., 2006). The relationship between the plastic response and indentation hardness is well known in the sense that strain hardening materials exhibit an increase in hardness due to plastic deformation. Regardless of the initial plastic strain, the indentation process itself will induce additional local plastic strain and causes a further increase in yield strength. In order to convert the micro-hardness measurements of Fig. 3 to local flow stress values as shown schematically in Fig. 1, the amount of local strain hardening induced by the micro-indent must be taken into account. This is done through the concept of representative plastic strain, ε_r, which is a measure of the average or "representative" plastic strain induced by a Vickers indent (Tabor, 1970). The representative plastic strain describes the extent that the average flow stress within the plastic zone exceeds the initial yield strength of the indented material as shown in Fig. 6a. Tabor (1970) suggested a representative strain value of 0.08 based on the hardness and flow curve data of copper and steel specimens. Since then, a large range of values for representative plastic strain have been suggested from 0.01 to 0.36 (Johnson, 1985; Dao et al., 2001; Chaudhri, 1998; Ogasawara et al., 2005; Cao and Huber, 2006; Tekkaya, 2000); but most of these are based on curve fitting of indentation loading curvatures of many materials. In general, the representative plastic strain defines one point on the flow curve that corresponds to $\sigma_r = \sigma(\varepsilon_r) = \frac{H}{C}$ where C is the constraint factor and H is the hardness of the virgin material and shown schematically in Fig. 6a. The representative plastic strain can also be used to estimate the hardness of a pre-deformed material (Fig. 6b) with an initial equivalent plastic strain ε_p, or simply

$$\begin{cases} H = C_j \sigma|_{\varepsilon=\varepsilon_r^j}, & \varepsilon_p^j = 0 \text{ (virgin material)} \\ H = C_j \sigma|_{\varepsilon=\varepsilon_r^j+\varepsilon_p^j}, & \varepsilon_p^j > 0 \text{ (predeformed material)} \end{cases} \tag{1}$$

where the values for ε_r and C may be a function of depth at a given location j within the PGM. This equation is similar to that used in Tabor (1970), except a material-dependent representative plastic strain is used here which was shown to be valid in Branch et al. (in press-a).

The representative plastic strain ε_r in this analysis is defined as the average plastic strain induced by a micro-Vickers indent, given by

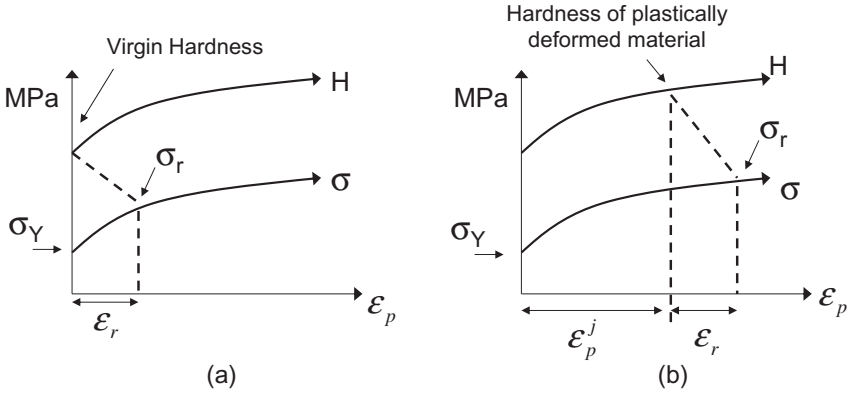

Fig. 6. Relationship between representative strain, flow stress and hardness for (a) virgin materials and (b) materials with initial plastic deformation, ε_p^j.

Please cite this article in press as: Branch, N.A., et al. Determination of constitutive response of plastically graded materials. Int. J. Plasticity (2010), doi:10.1016/j.ijplas.2010.09.001

$$\varepsilon_r = \frac{\sum \varepsilon_i V_i}{\sum V_i} \tag{2}$$

where ε_i is the equivalent plastic strain at the centroid of an elemental volume V_i within the plastic zone of a Vickers indent. This definition of *average* plastic strain was shown to be independent of yield strength and elastic modulus but dependent *only* on strain hardening exponent (n) by Jayaraman et al. (1998). This average plastic strain can also be used as a valid material-dependent representative plastic strain for Vickers indentation and independent of the initial plastic strain of an indented material (Branch et al., in press-a). This representative plastic strain is determined by modeling the plastic deformation due to Vickers indentation using finite element methods and then calculating the average volumetric plastic strain within its plastic zone on a per finite-element basis and Eq. (2). Calculated values for this average or representative plastic strain as a function of n can be found in (Jayaraman et al., 1998; Branch et al., in press-a) and will not be repeated here. For $n = 0.064$ of the core region, $\varepsilon_r = 0.052$ (Branch et al., in press-a) and its corresponding representative flow stress is 1506 MPa which has a constraint factor given by $C = \frac{H}{\sigma(\varepsilon_r)} = 2.82$.

For this specific PGM, the values of n at any given depth from the surface must be non-zero since an increase in hardness (thus strain hardening) has been observed in both plastically deformed PGMs as shown in Fig. 4. The strain hardening exponent of the core cannot be changed because it was experimentally determined from the compression test of the core region. Also note the maximum increase in hardness in Fig. 4 is approximately 45–50 Hv for both PGMs. This suggests that the strain hardening characteristics are similar throughout the PGM; therefore a constant strain hardening exponent of $n = 0.064$ (identical to the core region) can be used in this analysis. Recall that ε_r is a function of n only (Jayaraman et al., 1998), and therefore the value for representative plastic strain is also constant irrespective of the location within the PGM. The flow stress at the corresponding representative plastic strain defines one point on the material flow curve, $\sigma(\varepsilon_r) = \frac{H}{C}$ provided the values of C and H (Fig. 2) are known *a priori* (Tabor, 1970).

The relationship between hardness, yield strength, elastic modulus, and strain hardening exponent for power-law hardening materials was derived by Gao et al. (2006) using expanding cavity models in the following form:

$$\frac{H}{\sigma_y} = \frac{2}{3}\left\{\left(1 - \frac{1}{n}\right) + \left(\frac{3}{4} + \frac{1}{n}\right)\left(\frac{1}{3}\frac{E}{\sigma_y}\cot\alpha\right)^n\right\} \tag{3}$$

where α is the equivalent half cone angle for Vickers indenters and has a value of 70.3°. Because H and n are known for all depths, and assuming that $E = 200$ GPa for steel, the yield strength σ_y can then be determined from the above relationship for the entire PGM. The strength coefficient K as function of hardness (H) taken from Fig. 2 can now be calculated $K = E^n \sigma_y^{1-n}$ from the intersection of the elastic $\sigma_y = E\varepsilon_y$ and plastic $\sigma_y = K\varepsilon_y^n$ curves which vary with depth for a PGM. The resulting flow curves as a function of hardness is shown in Fig. 7a. The constraint factor $C = \frac{H}{\sigma(\varepsilon_r)}$ can now be calculated and shown in Fig. 7b. This data will be used in Eq. (1) to predict the Vickers hardness for a plastically deformed PGM using the equivalent plastic strain calculated by FE models described in the following section.

5. Finite element model

To determine if these flow curves accurately represent the plastic behavior of the PGM, the plastic strain induced by the macro-indent must be determined and then related to the micro-Vickers hardness measurements of Fig. 3 discussed earlier. The plastic strain is dependent on the material's ability to resist plastic deformation, i.e. its plastic response and strain hard-

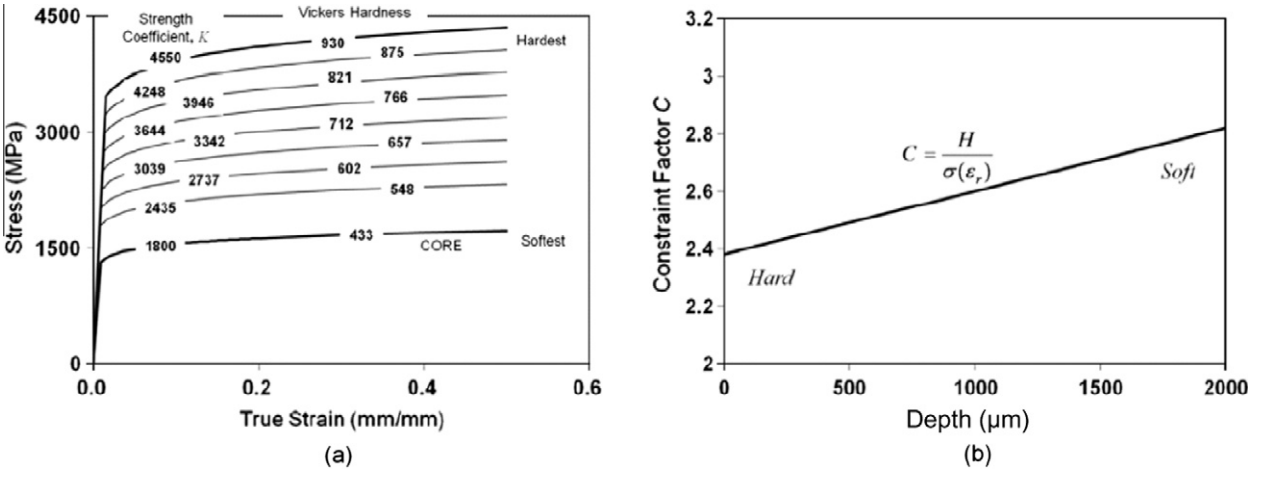

Fig. 7. (a) Power -law flow curves as function of hardness and (b) ratio of hardness to flow stress at the corresponding representative plastic strain.

ening characteristics. Determination of the plastic strain magnitude and its variation with depth beneath a Vickers indent is difficult, particularly for a PGM, thus finite element modeling provides a convenient way to compute the plastic strain variation beneath these macro-indents. In this axisymmetric model, a conical indenter with a half cone angle of 70.3° produces the same indentation area as a Vickers indent at a given indent depth. The indenter is considered rigid and therefore does not require a mesh. The indenter is displacement controlled to the same depth as in the experiment and then retracted to its original position. The indenter is given fixed rotational boundary conditions and allowed to translate normal to the specimen surface. Four thousand eight hundred four-node bilinear quadrilateral axisymmetric elements make up the Finite Element (FE) model with the finest mesh in the region closest to the indenter tip as shown in Fig. 8. The FE model is implemented in ABAQUS 6.7-1. The plastic response is governed by the von Mises (J2) yield criterion, associated flow rule, and isotropic hardening (ABAQUS Theory Manual). The flow curve variation of Fig. 7a is inserted into the finite element model via a gradient in applied temperature that is constant at a given depth but varies with depth in a similar fashion as the variation in hardness. Only the plastic response is assigned as a function of temperature with no thermal expansion properties defined. The macro-indentations of both hardest (Fig. 3a) and softest (Fig. 3b) PGMs are simulated to the same macro-indentation depths as the experiments. Similar axisymmetric modeling of indentation has been performed by Shi et al. (2010).

6. Results

The contours of constant equivalent plastic strains within the plastic zones as calculated by the FE models of both PGMs are shown in Fig. 9a. Note that the indentation on the hardest PGM surface has a shallower macro-indent depth (d = 118 μm

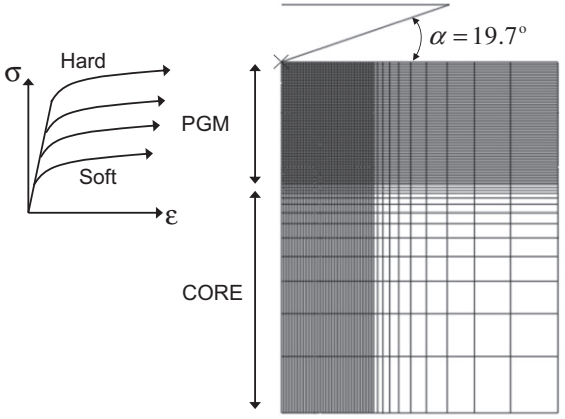

Fig. 8. FE model of the macro-Vickers indentation of a PGM.

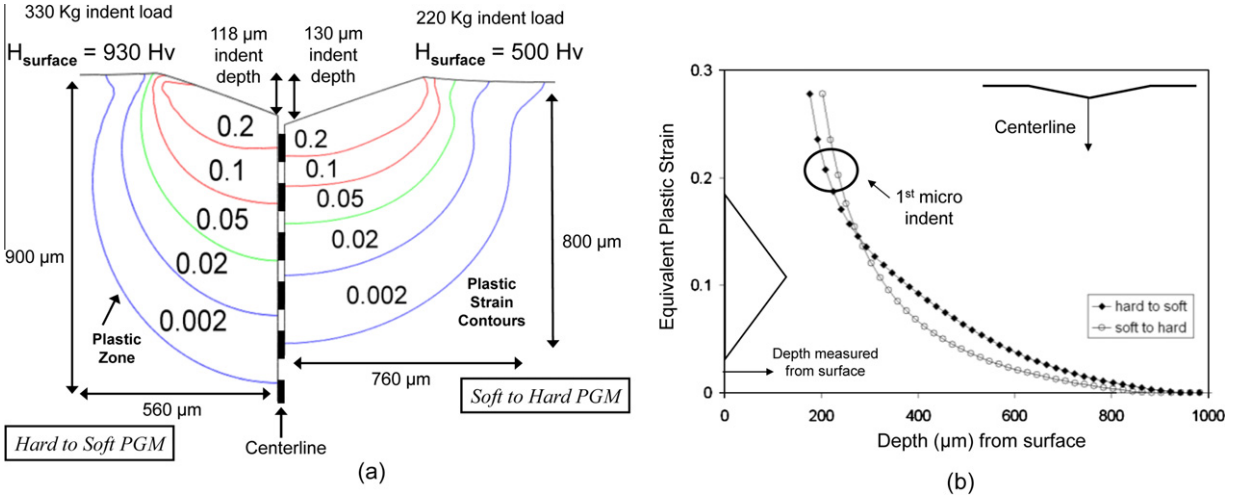

Fig. 9. (a) Equivalent plastic strain contours within the plastic zones induced by Vickers macro-indents on hardest and softest surfaces of the PGMs. (b) Comparison of the plastic strain magnitudes along centerlines of both PGMs as measured from material surface.

Please cite this article in press as: Branch, N.A., et al. Determination of constitutive response of plastically graded materials. Int. J. Plasticity (2010), doi:10.1016/j.ijplas.2010.09.001

at 330 Kg indent load) than the deeper macro-indent and lower indent load (230 Kg) on the softest PGM surface (d = 130 μm). However, the plastic zone for the hardest PGM is deeper and narrower than the plastic zone of the softest PGM. From these results it is inferred that the surface of the hardest PGM is more resistant to plastic deformation than its subsurface region and therefore forces plastic deformation to occur within the weaker, subsurface region. Although the softest PGM surface has a deeper macro-indent, it has a shallower and wider plastic zone because the softest-surface regions accommodate most of the plastic deformation while the subsurface regions are harder and more resistant to plastic deformation. These results show that distribution of plastic strain is more sensitive to the gradation in plastic response than the initial surface hardness. The equivalent plastic strains along the centerlines of both PGMs increase asymptotically as shown in Fig. 9b. This information will be used to predict the micro-Vickers hardness measurements of Fig. 4.

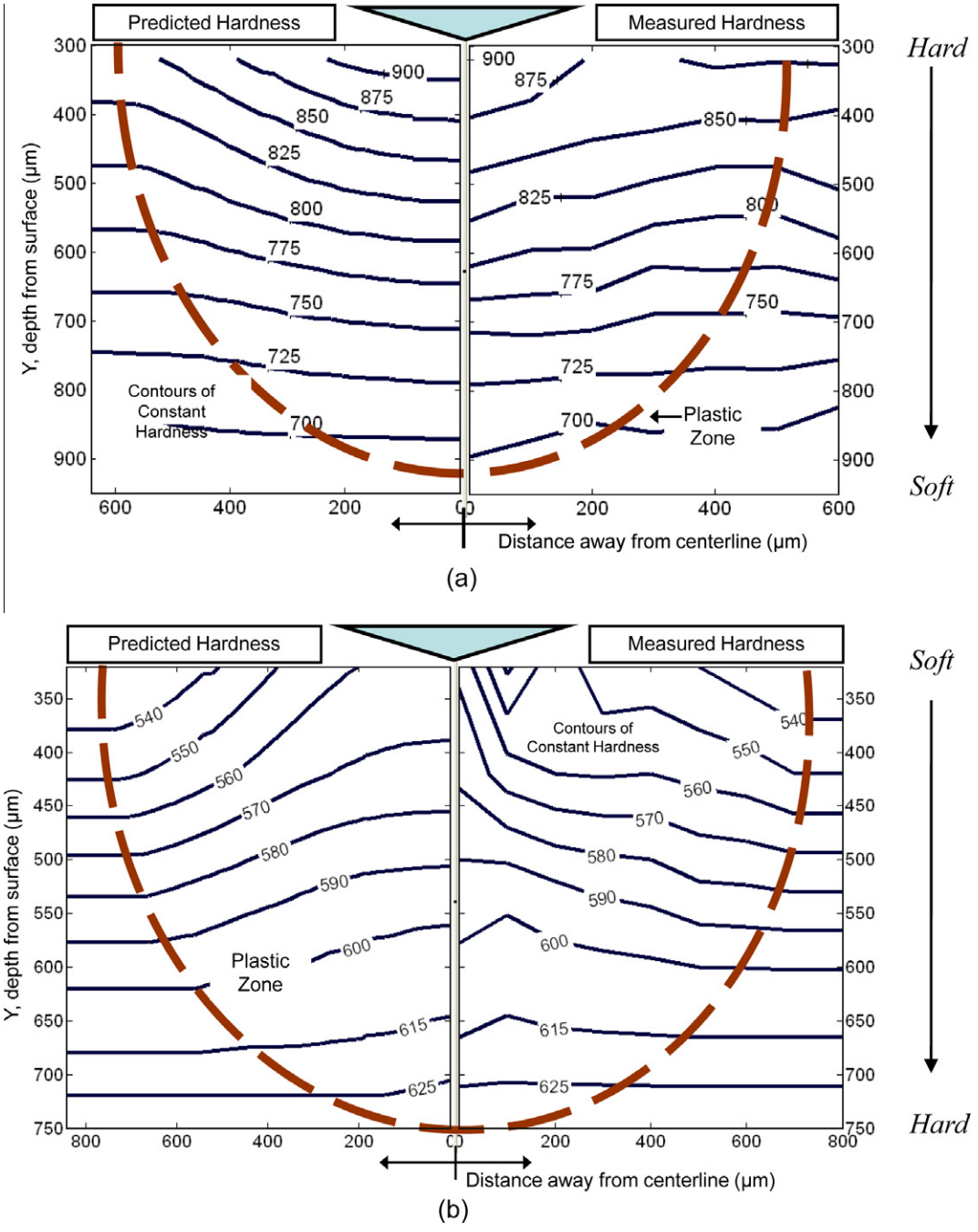

Fig. 10. Predicted versus measured micro-Vickers hardness values for the (a) hardest and (b) softest PGMs within the entire plastic zone of the macro-Vickers indentations.

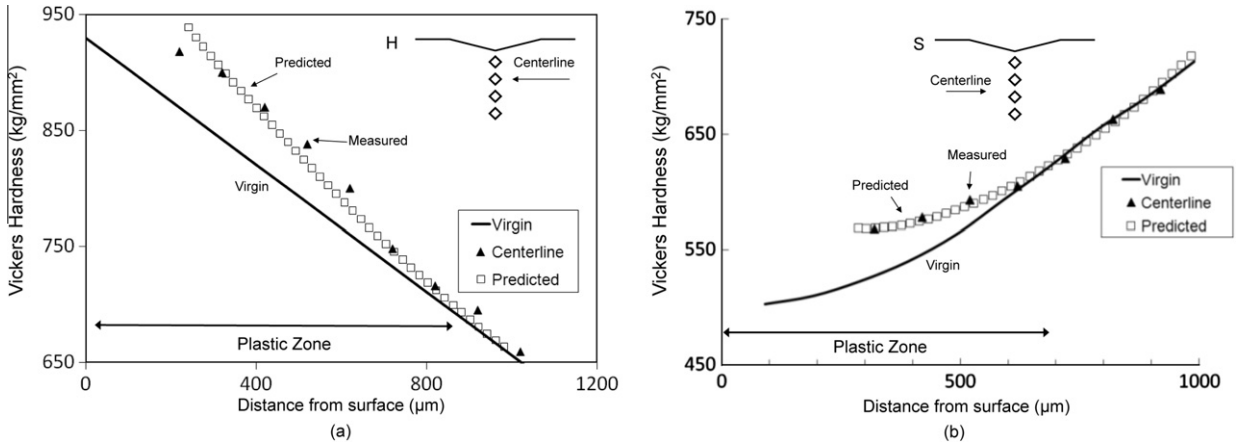

Fig. 11. Predicted versus measured micro-Vickers hardness values along the plastic zone's centerline for both (a) hardest and (b) softest PGMs.

The predicted micro-Vickers hardness at a given location j at any depth within the PGM plastic zone can now be determined by Eq. (1) where ε_p^j is the initial plastic strain induced by the macro-Vickers indent (Fig. 9) and ε_r^j is the representative plastic strain induced by the micro-Vickers indent at a given location. For the case where n is a constant 0.064 with depth, $\varepsilon_r^j = 0.052$ is constant with depth also. The flow stress that corresponds to the sum total of the representative plastic strain and equivalent plastic strain from Fig. 9 is calculated next for every point within the plastic zone. This information is used to predict the micro-Vickers hardness values per Eq. (1) and compared to the experimentally measured hardness in Fig. 3. Good agreement is seen between the predicted and measured hardness values beneath the macro-indents of both PGMs as shown in Fig. 10. The predicted micro-Vickers hardness values along the centerlines of both plastic zones are compared to the measured values shown earlier in Fig. 4 as shown again in Fig. 11 where a good match is also observed. The plastic zone size in these plots is estimated by comparing the micro-hardness values before and after the generation of the plastic strain, i.e., where the hardness contours merge with the virgin hardness at a given depth. Any discrepancy in the calculated plastic zone depth by the FE model is due to the sensitivity of the method in predicting hardness at low plastic strain, experimental scatter in the measured hardness, and the fact that the plastic zone boundary is defined at the 0.002 plastic strain contour. The predicted hardness is expected to have an increasing trend with respect to virgin hardness as it approaches the indenter tip because the flow stresses of the power-law plastic response increase with increasing plastic strain as seen in Fig. 9b. Consequently, this method of predicting Vickers hardness will predict higher hardness values in regions of high plastic strain which are closest to the indenter tip.

Note that there is good agreement between the measured and predicted hardness values for both PGMs irrespective of the increasing or decreasing hardness gradients below the surface. This validates the assumption of constant strain hardening exponent with depth for this specific case-hardened stainless steel. Since the graded layer gradually merges with the core material, the assumption of constant strain hardening exponent for the PGM is logical. A different set of flow curves would predict different micro-Vickers hardness values within the plastic zone of the macro-Vickers indent for the same *macro-indent depths*. Although the PGM used in this analysis was shown to have a constant strain hardening exponent, this method can be applied to PGMs that have variations in n as well because the expanding cavity model derived by Gao et al. (2006) takes into account the dependence of hardness on n. The dependence of the predicted increase in hardness on variations in n has been systematically studies for both non-graded and plastically graded materials in Branch et al. (in press-b). However, in the current analysis, the availability of hardening exponent for the core region makes the analysis simpler.

7. Summary

The proposed method predicts the experimentally measured increase in indentation hardness of a plastically deformed PGM, and in the process, extracts the stress-strain response of the graded material as a function of depth. This method utilizes proven concepts regarding representative plastic strain (Jayaraman et al., 1998, Branch et al., in press-a), constraint factor (Gao et al., 2006), and the micro-indentation mapping of a plastically deformed region (Srikant et al., 2006; Chaudhri, 1998; Koeppel and Subhash, 1999). These concepts are combined to convert the measured Vickers hardness values to flow stresses that must fall on the flow curve at a specified depth within the deformed PGM. The corresponding plastic strain is determined by FE modeling of the macro indentation process. The procedure developed is very general and applicable for PGMs with increasing or decreasing hardness gradient. This method is convenient because it does not require instrumented indentation devices or curve fitting of many complex dimensionless functions. The proposed method is applicable for other modes of plastic deformation as well, but macro-Vickers indents were chosen here due to their ease of use and availability. Such a procedure is useful to customize a PGM to meet the specific needs of an engineering application, such as surface engineering of new graded materials with optimized hardness profiles to maximize component tribological performance.

Please cite this article in press as: Branch, N.A., et al. Determination of constitutive response of plastically graded materials. Int. J. Plasticity (2010), doi:10.1016/j.ijplas.2010.09.001

In summary, the variation in constitutive response within the case-hardened region of commercially available P675 stainless steel was determined. Both micro- and macro-Vickers indentation and finite element modeling were utilized to predict the increase in hardness within a plastically deformed PGM. It was shown that the relative depth and width of the plastic zone from macro Vickers indentation is indicative of whether the hardness gradient is increasing or decreasing with depth. The PGM used in this analysis was determined to have a linear variation in yield strength and hardness, but a constant strain hardening exponent.

Acknowledgements

This work was partially supported by the National Science Foundation Award CMMI-0927849 under program officer Dr. Clark V. Cooper, and by the Timken Company, Canton, OH, through the US Air Force/VAATE Contract #: F33615-03-D-2353-003. The authors express their gratitude to Dr. Nelson Forster, Mr. Vaughn Svendsen, and Dr. Lewis Rosado of AFRL for their contributions to this project. Thanks also to Dr. William Hannon, Dr. Liz Cooke, and Mr. Bob Wolfe of the Timken Co. for their continued support of this work. Sincere thanks to Mr. Bill Ogden, Dr. Herb Chin, and Mr. David Haluck of Pratt & Whitney for their interest and support of this research.

References

Anand, L., Ames, N.M., 2006. On modeling the micro-indentation response of an amorphous polymer. Int. J. Plasticity 22, 1123–1170.
Boyer, H., 1987. Case Hardening of Steels. ASTM, Metals Park, OH.
Branch, N.A., Subhash, G., Arakere, N.K., Klecka, M.A., in press-a. Material dependent representative plastic strain for the prediction of indentation hardness. Acta Mater.
Branch, N.A., Subhash, G., Klecka, M.A., Arakere, N.K., in press-b. A new reverse analysis to determine the constitutive response of plastically graded steels. Int. J. Solids Struct.
Cao, T., Huber, N., 2006. Further investigation on the definition of the representative strain in conical indentation. J. Mater. Res. 21 (7).
Cao, Y.P., Lu, J., 2004. A new scheme for computational modeling of conical indentation in plastically graded materials. J. Mater. Res. 19 (6).
Chaudhri, M.M., 1998. Subsurface strain distribution around Vickers hardness indentations in annealed polycrystalline copper. Acta Mater. 46 (9).
Choi, I.S., Dao, M., Suresh, S., 2008a. Mechanics of indentation of plastically graded materials I: Analysis. J. Mech. Phys. Solids 56.
Choi, I.S., Detor, A.J., Schwaiger, R., Dao, M., Schuh, C.A., Suresh, S., 2008b. Mechanics of indentation of plastically graded materials II: Experiments on nanocrystalline alloys with grain size gradients. J. Mech. Phys. Solids 56.
Cordill, M.J., Lund, M.S., Parker, J., Leighton, C., Nair, A.K., Farkas, D., Moody, N.R., Gerberich, W.W., 2009. The Nano-Jackhammer effect in probing near-surface mechanical properties. Int. J. Plasticity 25, 2045–2058.
Dao, M., Chollacoop, N., Van Vliet, K.J., Venkatesh, T.A., Suresh, S., 2001. Computational modeling of the forward and reverse problems in instrumented sharp indentation. Acta Mater. 49.
Desault Systemes, 2007. ABAQUS Theory Manual, Dessault Systemes, Providence, RI.
Fischer-Cripps, A.C., 2003. Analysis of instrumented indentation test data for functionally graded materials. Surf. Coat. Technol. 168.
Fleck, N.A., Hutchinson, J.W., 2001. A reformulation of strain gradient plasticity. J. Mech. Phys. Solids. 49, 2245–2271.
Fleck, N.A., Muller, G.M., Ashby, M.F., Hutchinson, J.W., 1994. Strain gradient plasticity: Theory and experiment. Acta Metall. Mater. 42, 475.
Gao, X.L., Jing, X.N., Subhash, G., 2006. Two new expanding cavity models for indentation deformations of elastic strain hardening materials. Int. J. Solids Struct. 43.
Giannakopoulos, A.E., 2002. Indentation of plastically graded substrates by sharp indenters. Int. J. Solids Struct. 39.
Gu, Y., Nakamura, T., Prchlik, L., Sampath, S., Wallace, 2003. Micro-indentation and inverse analysis to characterize elastic-plastic graded materials. J. Mater. Sci. Eng. A345.
Haj-Ali, R., Kim, H.K., Koh, S.W., Saxena, A., Tummala, R., 2008. Nonlinear constitutive models from nanoindentation tests using artificial neural networks. Int. J. Plasticity 24, 371–396.
Huang, Y., Qu, S., Hwang, K.C., Li, M., Gao, H., 2004. A conventional theory of mechanism based strain gradient plasticity. Int. J. Plasticity. 20, 753–782.
Jayaraman, S., Hahn, G.T., Oliver, W.C., Rubin, C.A., Bastias, P.C., 1998. Determination of monotonic stress strain curve of hard materials from ultra low load indentation tests. Int. J. Solids Struct. 35 (56).
Johnson, K.L., 1985. Contact Mechanics. Cambridge University Press.
Koeppel, B.J., Subhash, G., 1999. Characteristics of residual plastic zone under static and dynamic Vickers indentations. Wear 224, 56–67.
Miyamoto, Y., Kaysser, W.A., Rabin, B.H., 1999. Functionally Graded Materials: Design, Processing, and Applications. Springer.
Nakamura, T., Wang, T., Sampath, S., 2000. Determination of properties of graded materials by inverse analysis and instrumented indentation. Acta Mater. 48.
Nayebi, A., El Abdi, R., Bartier, O., Mauvoisin, G., 2002. Hardness profile analysis of elasto-plastic heat treated steels with a gradient in yield strength. Mater. Sci. Eng. A333.
Ogasawara, N., Chiba, N., Chen, X., 2005. Representative strain of indentation analysis. J. Mater. Res. 20 (8).
Qu, S., Huang, Y., Pharr, G.M., Hwang, K.C., 2006. The indentation size effect in the spherical indentation of iridium: A study via the conventional theory of mechanism-based strain gradient plasticity. Int. J. Plasticity 22, 1265–1286.
Abu Al-Rub, Rashid K., Voyiadjis, George Z., 2004. Analytical and experimental determination of the material intrinsic length scale of strain gradient plasticity theory from micro- and nano-indentation experiments. Int. J. Plasticity 20, 1139–1182.
Shi, Z., Feng, X., Huang, Y., Xiao, J., Hwang, K.C., 2010. The equivalent axisymmetric model for Berkovich indenters in power-law hardening materials. Int. J. Plasticity 26, 141–148.
Smith, C.S., 1960. A History of Metallography. MIT Press, Cambridge, MA.
Srikant, G., Chollacoop, N., Ramamurty, U., 2006. Plastic strain distribution underneath a Vickers indenter: Role of yield strength and work hardening exponent. Acta Mater. 54.
Suresh, S., Mortensen, A., 1998. Fundamentals of Functionally Graded Materials. Maney Materials Science.
Tabor, D., 1970. The Hardness of Solids. Review of Physics in Technology 1, 145–179.
Tekkaya, A.E., 2000. An improved relationship between Vickers hardness and yield stress for cold formed materials and its experimental verification. CIRP Ann. – Manufact. Technol. 1 (1), 205–208.
Zhang, F., Saha, R., Huang, Y., Nix, W.D., Hwang, K.C., Qu, S., Li, M., 2007. Indentation of a hard film on a soft substrate: Strain gradient hardening effects. Int. J. plasticity 23, 25–43.

Please cite this article in press as: Branch, N.A., et al. Determination of constitutive response of plastically graded materials. Int. J. Plasticity (2010), doi:10.1016/j.ijplas.2010.09.001